

Blowing-induced boundary-layer separation of shear-thinning fluids

P. P. Dabrowski and J. P. Denier

Department of Applied Mathematics
 Adelaide University, South Australia, 5005 AUSTRALIA

Abstract

We consider the problem of blowing-induced boundary-layer separation of a general class of shear-thinning fluids. A uniform blowing velocity is prescribed at the surface of a flat plate. In the case of a Newtonian fluid this flow separates at a finite distance downstream from the leading edge of the plate. In order to quantify separation for a non-Newtonian fluid, the boundary-layer equations, in both similar and non-similar form, are solved. Our results demonstrate that shear-thinning fluids can act as a useful deterrent of flow separation.

Introduction

Boundary-layer separation is one of the fundamental problems of fluid dynamics. The potential benefits in controlling flow separation have driven much of recent work on this topic. Here we consider the problem of the constant rate injection of a shear-thinning fluid into a laminar boundary-layer flow over a flat plate; the boundary-layer fluid and the injection fluid are taken to be identical in all respects.

Wu & Thompson [9] demonstrated that the boundary-layer approximation is valid for shear-thinning fluids down to Reynolds number of the order of thousands. This work was confined to attached flat-plate flows and did not consider the question of flow separation. In the case of Newtonian fluids, boundary-layer separation induced by fluid injection has received considerable attention in the past thirty years. The early work of Catherall *et al.* [3] considered the problem of the separation of the flow of a Newtonian flat-plate boundary layer induced by blowing through the plate. Their numerical solution of Prandtl's boundary-layer equations demonstrated the structure of the flow at the onset of separation. From these results they were able to deduce that at the point of vanishing skin-friction the flow develops in such a way that

$$c_f = \nu \left. \frac{\partial u}{\partial y} \right|_{y=0} \sim \left(\frac{x^*}{\ln(1/x^*)} \right)^2 \quad \text{as } x^* = x_s - x \rightarrow 0$$

where x_s is the point of separation. Thus the flow terminates in a singularity at the point of separation. This singularity is different from the classical Goldstein singularity [5] which exhibits an algebraic dependency on x^* in the limit $x^* \rightarrow 0$. This work was subsequently extended by a number of authors to supersonic flows [8] and injection [7] through a finite slot (see [2] for a recent review on boundary-layer separation).

The boundary-layer flow of shear-thinning fluids can be characterised by the fact that the shear stress is reduced as compared to an otherwise equivalent Newtonian flow [1]. This then suggests that the onset of flow separation will be affected, perhaps quite dramatically, by the introduction of a non-Newtonian fluid into the flow. Such is the subject of the present investigation.

Formulation

Consider then the boundary-layer flow of a non-Newtonian fluid over a permeable flat plate through which fluid is injected at a constant rate. For definiteness we will take as our model non-Newtonian fluid one in which the shear stress is related to the rate-of-strain via the power-law model

$$\tau = K\dot{\gamma}^n,$$

where $\dot{\gamma}$ is the rate-of-strain given by

$$\dot{\gamma} = \sqrt{\left(\frac{\partial U}{\partial \tilde{y}} \right)^2 + \left(\frac{\partial V}{\partial x} \right)^2}.$$

We focus on shear-thinning fluids for which the fluid index $n < 1$. Here x and \tilde{y} are Cartesian coordinates aligned along and normal to the plate, respectively, and U, V are the corresponding components of the velocity field. All lengths have been non-dimensionalized with respect to a characteristic length scale L and speeds with respect to a characteristic speed U_∞ .

In order to pose the problem within a boundary-layer context we must restrict our attention to a regime in which the wall-normal blowing (or injection) speed is of size $O(Re^{-1/(n+1)})$ (see below). Introducing the boundary-layer variables

$$y = Re^{1/(n+1)}\tilde{y}, \quad V = Re^{-1/(n+1)}v(x, y), \quad U = u(x, y)$$

we find the boundary-layer equations can be written as

$$\frac{\partial u}{\partial x} + \frac{\partial v}{\partial y} = 0, \tag{1a}$$

$$u \frac{\partial u}{\partial x} + v \frac{\partial u}{\partial y} = -u_e(x) \frac{du_e}{dx} + n \left(\frac{\partial u}{\partial y} \right)^{n-1} \frac{\partial^2 u}{\partial y^2}, \tag{1b}$$

which must be solved subject to boundary conditions

$$u = v - C(x) = 0 \quad \text{at } y = 0, \tag{2a}$$

$$u = u_e(x) \quad \text{as } y \rightarrow \infty. \tag{2b}$$

In arriving at (1b) we have used the fact that under the boundary-layer approximation the rate-of-strain reduces to

$$\dot{\gamma} = Re^{1/(n+1)} \frac{\partial u}{\partial y}.$$

Self-similar flows

In general it is not possible for the flow to develop in a self-similar fashion unless the blowing velocity is chosen to take on a particular functional form in terms of the distance x from the leading edge of the plate. To see this we seek a general solution in similarity form

$$u = x^m f'(\eta), \quad v = x^{s+m-1} [s\eta f' - (s+m)f],$$

where

$$\eta = y/(\alpha x^{-s}).$$

For such a similarity form to exist the blowing velocity must be prescribed by

$$v(0) = C(x) = C_0 x^{s+m-1},$$

and the similarity index s given by

$$s = \frac{1 + m(n-2)}{1+n} \quad \text{with} \quad \alpha = n^{1/(n+1)}.$$

The equation governing the self-similar flow is then

$$(f'')^{n-1} f''' = m(f')^2 + m - (s+m)ff'', \quad (3)$$

which must be solved subject to the boundary conditions

$$f(0) = -\frac{C_0}{\alpha(s+m)}, f'(0) = 0 \quad f'(\infty) = 1. \quad (4)$$

Note that the case of a flat-plate boundary layer is recovered by setting $m = 0$ in equation (3).

Equation (3) was solved using a simple shooting method which employed a fourth-order Runge-Kutta quadrature scheme. After some experimentation the integration step-size was chosen to be $\Delta\eta = 0.02$. Near the point of vanishing skin-friction the behaviour of the velocity field in the far field was monitored to ensure that f' had the correct asymptotic behaviour (i.e. $f' \rightarrow 1 + \exp.$ small terms). We therefore monitored the behaviour of f'' to ensure that it approached zero in the far-field. This dictated setting the far-field boundary condition at $\eta_\infty = 200$ thus giving 10^5 points in the η direction.

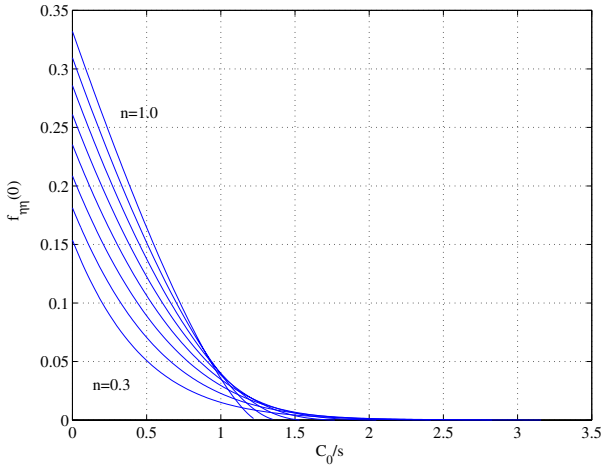


Figure 1: Plot showing the dependency of the reduced skin-friction on C_0/s for values of $n = 1, 0.9, \dots, 0.3$.

The results of this calculation, for the case of Blasius-like flow $m = 0$, are presented in Figs. 1 and 2. Figure 1 shows plots of the reduced skin-friction $f_{\eta\eta}(0)$ versus the normalized blowing velocity C_0/s for values of the power-law index n ranging from 1 to 0.3. The zero-blowing results $C_0 = 0$ agree with the earlier results of Acrivos *et al.* [1]. In all cases presented, increasing the magnitude of C_0/s leads to separation, defined in this instance as the point at which the wall shear $f_{\eta\eta}(0) = 0$. This is readily seen in Fig. 2 where we plot the value of C_0/s at which separation

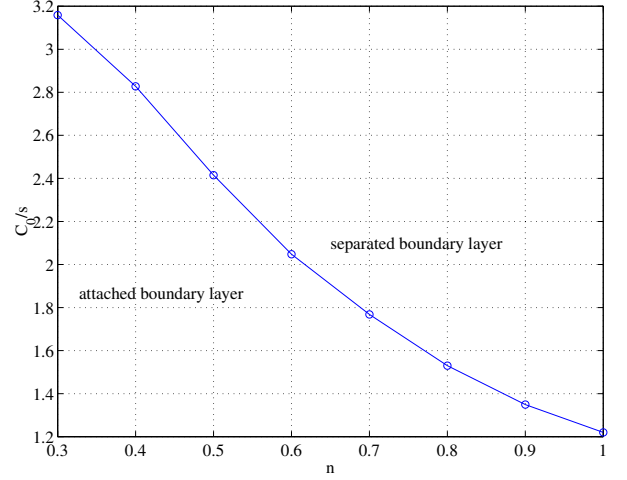


Figure 2: Plot showing the dependency of the “point of separation” on the power-law index n . Here the boundary layer is deemed to have separated (i.e. a point of vanishing skin-friction is attained) when $f''(0) < 1.0 \times 10^{-4}$.

occurs versus n . Flows whose parameters fall in the region above the curve are separated (or detached). These results hint at the separation-delaying potential of shear-thinning fluids. However, because of the nature of these results (being for a blowing velocity $v(0, x) = C_0 x^{s-1}$), it is difficult to interpret them for the more physically realistic flow of constant blowing. Although similarity solutions do exist for this case (we have the requirement that $m = 1 - s$ in (3)) the simplest case of uniform flow over a flat plate with uniform injection of fluid at the plate cannot be described via a similarity solution. We are thus forced to solve the full boundary-layer equations (1) numerically. We now turn our attention to this task.

Non-self-similar flows

In order to place the system (1) into a form that is suitable for computational purposes we define new independent variables $\xi = (nx)^{n/(n+1)}$, the streamwise coordinate, and $\eta = y/(nx)^{-1/(n+1)}$, the wall-normal coordinate. The x -momentum equation (1b) becomes

$$\left(\frac{\partial u}{\partial \eta}\right)^{n-1} \frac{\partial^2 u}{\partial \eta^2} = \frac{u}{n+1} \left[n\xi \frac{\partial u}{\partial \xi} - \eta \frac{\partial u}{\partial \eta} \right] + \frac{1}{n} \xi v \frac{\partial u}{\partial \eta}, \quad (5)$$

while the continuity equation (1a) reduces to

$$\frac{1}{n} \xi \frac{\partial v}{\partial \eta} = \frac{1}{n+1} \left[\eta \frac{\partial u}{\partial \eta} - n\xi \frac{\partial u}{\partial \xi} \right]. \quad (6)$$

Integrating (6) with respect to η gives

$$\frac{1}{n} \xi v = \frac{1}{n+1} \left[\eta u - \int_0^\eta \left(n\xi \frac{\partial u}{\partial \xi} + u \right) d\eta \right] + \frac{1}{n} \xi C, \quad (7)$$

where the boundary condition $v = C$ on $\eta = 0$ has been used to determine the constant of integration. Combining equations (5) and (7) produces the following integro-differential form of the boundary-layer equations

$$\left(\frac{\partial u}{\partial \eta}\right)^{n-1} \frac{\partial^2 u}{\partial \eta^2} + \left[\frac{1}{n+1} \int_0^\eta \left(n\xi \frac{\partial u}{\partial \xi} + u \right) d\eta - \frac{1}{n} \xi C \right] \frac{\partial u}{\partial \eta} - \frac{n}{n+1} \xi u \frac{\partial u}{\partial \xi} = 0. \quad (8)$$

Setting $n = 1$ (the case of a Newtonian fluid) we find equation (8) reduces to that solved by Catherall *et al.* [3].

The numerical scheme

Equation (8) was solved using the method employed by Catherall *et al.* [3]. Second-order centred differences were used to replace derivatives with respect to η and ξ . The discretization in the ξ direction exploits the parabolic nature of the boundary-layer equations and allows for an efficient marching scheme in the ξ direction to be set-up. The resulting numerical scheme is fully implicit and consists of a set of J non-linear algebraic equations. These equations relate the J pivotal values u_j at the current ξ station to the J pivotal values \bar{u}_j at the previous ξ station:

$$\begin{aligned} & \hat{u}_{j+1}^{(k)} - 2\hat{u}_j^{(k)} + \hat{u}_{j-1}^{(k)} + \left(\frac{\hat{u}_{j+1}^{(k)} - \hat{u}_{j-1}^{(k)}}{2h} \right)^{2-n} \times \\ & \left\{ \frac{h^3}{n+1} T_{r=0}^j \left(2n\hat{\xi} \frac{[\hat{u}^{(k)} - \bar{u}]_r}{\Delta\xi} + \hat{u}_r^{(k)} \right) - \frac{h^2}{n} \hat{\xi} C \right\} \\ & - \frac{2nh^2 \hat{\xi}}{(n+1)\Delta\xi} \hat{u}_j^{(k)} [\hat{u}^{(k)} - \bar{u}]_j \left(\frac{\hat{u}_{j+1}^{(k-1)} - \hat{u}_{j-1}^{(k-1)}}{2h} \right)^{1-n} = 0 \end{aligned} \quad (9)$$

for $j = 1, \dots, J$,

where the circumflex denotes the arithmetic mean of values at the current and previous ξ stations, T denotes the trapezoidal sum with the first and last terms halved, and k is the iteration count. At each ξ station the boundary conditions $u_0 = 0$ and $u_{J+1} = 1$, corresponding to no-slip along the plate and matching to the free-stream velocity in the limit $\eta = \eta_{max} \gg 1$, were explicitly satisfied. The J nonlinear algebraic equations (9) were solved using a J -dimensional Newton iteration method. At each level of iteration k the linear system of J equations was solved by Gaussian elimination. In all results reported here the injection velocity, denoted by C in (9), is taken to be constant along the entire plate and was set equal to unity.

A uniform step-size in ξ was adopted with the step-size, $\Delta\xi$. After some experimentation we chose $\Delta\xi = 1 \times 10^{-4}$. In the wall-normal direction the grid was uniform and the spacing h was set to 0.01. To commence the marching an initial velocity profile at $\xi = 0$ is needed. These were calculated by solving a Blasius-like ordinary differential equation, (3) with $m = 0$, for different values of the fluid index n . To monitor the progress of the calculations and to determine the location of the point of separation the reduced skin friction, which is given by $\frac{\partial u}{\partial y}|_{y=0}$, is calculated. At each ξ station a value for the reduced skin friction is calculated using a second-order accurate finite-difference approximation. When the value of the reduced skin friction falls below a certain threshold, 1×10^{-4} in this case, separation of the flow was deemed to have occurred and the computations were terminated.

Results and Discussion

The results from our calculations are presented in Figs. 3 – 5. Fig. 3 shows a plot of the streamwise location x_s at which the flow separates as a function of the fluid index n . As n is decreased, so that the shear-thinning nature of the fluid increases, the point of separation moves further from the leading edge of the plate. It is perhaps not surprising that the variation of x_s with n is non-linear given the nonlinear dependency of the governing

equations on n . In order to interpret these results we slightly recast our problem and suppose that in our non-dimensionalisation of the streamwise variable we take our characteristic length scale L to be equal to the length of the plate. A non-dimensional streamwise variable $x = 1$ now corresponds to the trailing edge of the plate.[‡] We can then determine the value of n for which the boundary layer remains attached along the whole length of the plate (for the constant value of the blowing velocity considered here $C = 1$). From Fig 3, reading off the value of n for which $x_s = 1$, we find for $n < 0.89$ the flow remains attached (unseparated) along the whole length of the plate.

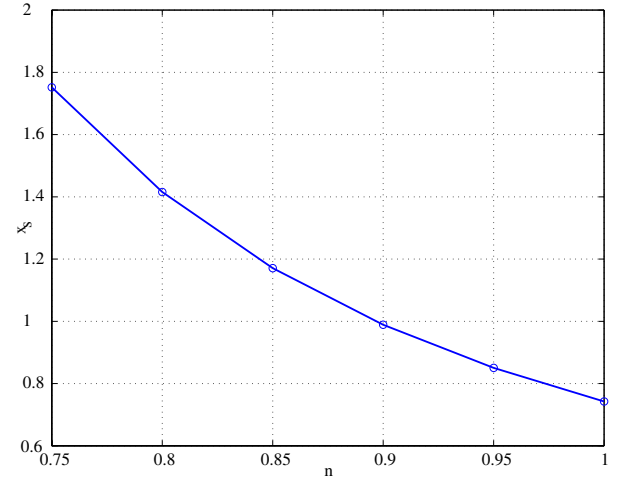


Figure 3: Plot showing the location of the separation point, x_s , versus the fluid index, n .

During our calculations we encountered a significant dependency of the location of the separation point on the choice of the position η_∞ at which the far-field boundary condition was applied. If $\eta_\infty = J\Delta\eta$ was not selected carefully, so as to ensure that the streamwise velocity satisfies its correct asymptotic boundary condition, the numerical scheme converged to an invalid velocity profile and would generally under-predict the point of separation. In Fig. 4 we present velocity profiles at the numerically determined value of separation $x = x_s$. Here we see that, for the range of n -values considered, $u \rightarrow 1$ and $u_\eta \rightarrow 0$ at $\eta = \eta_\infty$. As the value of n is decreased the value of η_∞ was increased. This is a direct consequence of the fact that the boundary-layer thickness increases with decreasing n . This computational requirement of η_∞ on n places a heavy computational burden on the scheme that we have used if we are to retain sufficient accuracy in the η direction. It also provides a lower bound on the values of n which we were able to study; with the computational resources available $n = 0.75$ was the limiting case.

In Fig. 5 we present plots of the streamwise velocity field versus η for values of x ranging from $x = 0$ (the starting profile) to $x = x_s$ for the particular case of fluid index $n = 0.75$. This demonstrates how the velocity profile develops as the marching scheme progresses along the plate. As x increases the boundary layer thickens. Further down

[‡]Of course, the calculations must terminate at that point as the boundary layer equations are no longer valid in the wake, or for that matter in the vicinity of the trailing edge.

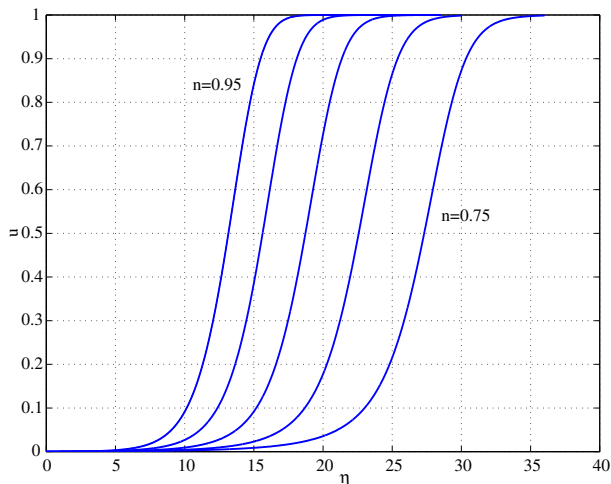


Figure 4: Plot of streamwise velocity u versus η at the point of separation for different values of the fluid index n .

the plate the flow shows quite a sudden and dramatic growth of the boundary layer as the point of vanishing skin friction (the separation point) is approached. Such blow-off of the boundary layer is typical when injection of fluid is present. We also note that these results serve to provide confirmation that the flow does not develop in a self-similar fashion when the blowing velocity is constant.

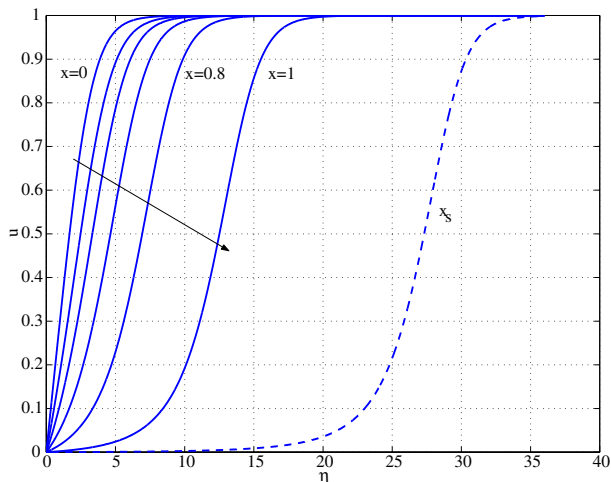


Figure 5: Plot of the streamwise velocity versus η at different locations, $x = 0, 0.2, 0.4, 0.6, 0.8, 1.0$ and $x = x_s$, along the plate for a fluid with index $n = 0.75$.

Conclusions

We have considered the problem of blowing-induced boundary-layer separation for a general class of non-Newtonian fluids whose shear stress is modelled by a power-law constitutive relation. For a fixed value of the blowing velocity the effect of decreasing the fluid index n is to shift the point of separation further downstream from the leading edge of the plate. This result clearly demonstrates the separation-delaying effectiveness of shear-thinning fluids.

The analysis was based upon the assumption that the

fluid within the boundary layer and the injected fluid were identical. This somewhat restrictive assumption could, of course, be relaxed by considering the problem as a two-component flow in which the upper fluid is Newtonian and the lower fluid is non-Newtonian. Such a formulation would resolve the question as to how a film of shear-thinning fluid will affect the dynamics of the boundary layer.

The results presented above have been obtained under the assumption that the boundary-layer flow remains laminar *prior* to separation. However, associated with the onset of boundary-layer separation the flow will develop points of inflexion at which $u_{yy}(y_c, x) = 0$; see Fig. 5. In this case the flow becomes susceptible to the short wavelength instabilities known as Rayleigh waves [4]. Whether, or where, the flow does develop these short-wavelength instabilities and how their growth rates are modified by the non-Newtonian nature of the underlying boundary-layer flow is, as yet, unknown. We hope to be able to answer these questions in the near future.

Acknowledgements

All calculations were carried out on an SGI Power Challenge operated by the South Australian Centre for High Performance Computing. J.P.D. would like to thank Stephen Otto for several useful discussions concerning this topic.

References

- [1] A. Acrivos, M.J. Shah and E.E. Petersen, Momentum and Heat Transfer in Laminar Boundary-Layer Flows of Non-Newtonian Fluids Past External Bodies, *AIChE J.*, **6**, (1960) 312–317.
- [2] S. N. Brown, *Laminar Boundary Layers and Separation*, Research Trends in Fluid Dynamics, AIP (1996) 43–54.
- [3] D. Catherall, K. Stewartson and P. G. Williams, Viscosity flow past a flat plate with uniform injection, *Proc. R. Soc. Lond. A* 284 (1965) 370–396.
- [4] P.G. Drazin and W.H. Reid *Hydrodynamic Stability*, C.U.P. (1979).
- [5] S. Goldstein, On laminar-boundary layer flow near a point of separation *Quart. J. Mech. Appl. Math.* **1** (1948) 43–69.
- [6] H. Schlichting, *Boundary-Layer Theory*, McGraw-Hill, Inc. (1979) 467.
- [7] F. T. Smith, On the High Reynolds number theory of laminar flows, *IMA J. Appl. Math.* **28** (1982) 207–281.
- [8] F. T. Smith and K. Stewartson, Plate-injection into a separated supersonic boundary layer, *J. Fluid Mech.*, **58** (1973) 143–158.
- [9] J. Wu and M.C. Thompson, Non-Newtonian shear-thinning flows past a flat plate, *J. Non-Newtonian Fluid Mech.*, **66** (1996) 127–144.